Journal of Chromatography, 598 (1992) 169–180
Elsevier Science Publishers B.V., Amsterdam

CHROM. 24 030

Protein chromatography using a continuous stationary phase

Yiqi Yang☆

Textile Science, Department of Consumer Sciences and Retailing, Purdue University, West Lafayette, IN 47907 (USA)

Ajoy Velayudhan

Laboratory of Renewable Resources Engineering, Purdue University, West Lafayette, IN 47907 (USA)

Christine M. Ladisch

Textile Science, Department of Consumer Sciences and Retailing, Purdue University, West Lafayette, IN 47907 (USA)

Michael R. Ladisch*

Laboratory of Renewable Resources Engineering and Department of Agricultural Engineering, Purdue University, West Lafayette, IN 47907 (USA)

(First received April 3rd, 1991; revised manuscript received November 21st, 1991)

ABSTRACT

A continuous stationary phase consisting of yarns woven into a fabric is rolled and packed into mechanically stable liquid chromatography columns. This work utilized yarns having a characteristic width of 200–400 μm, made from 10–20-μm fibers consisting of 95% poly(*m*-phenylene isophthalamide) and 5% poly(*p*-phenylene terephthalamide). Although loadings on this stationary phase were low at 4 mg/g for bovine serum albumin and 6 mg/g for β-galactosidase, this material shows the interesting characteristic of a leveling off of plate height at mobile phase velocities of 30–80 cm/min. This phenomenon is explained on the basis of a coupling argument whereby a fraction of the mobile phase flows through the intramatrix pore space, and convective transport through the pore space dominates transport by diffusion. A modified Van Deemter expression is derived and shown to fit plate height data for polyethylene glycol standards having molecular weights of 200 and 20 000. The characteristics of this continuous stationary phase at high eluent velocities are discussed and conditions which give separation of immunoglobulin G, bovine serum albumin, insulin and β-galactosidase in 12 min are described.

INTRODUCTION

Separation costs in the manufacture of proteins and other biotechnology products are estimated to be 40% or more of the production cost [1]. Key factors which improve the cost-effectiveness of a chromatographic process are reduction of the number of steps, automation to reduce labor costs, and reduction of media costs [2,3]. Improvements are still needed in the separations technology itself, particularly in reducing residence time.

Protein–stationary phase interactions and retention behavior reflect microscopic phenomena associated directly with the chemistry of the stationary phase, and are thus an important area of study. However, a successful process-scale system must

☆ Present address: Division of Consumer Sciences, 905 South Goodwin, University of Illinois, Champaign/Urbana, IL 61801, USA.

0021-9673/92/$05.00

also provide high mass transfer rates at low pressure drop. This is equivalent to a high ratio of mass to momentum transfer. In this context, Gibbs and Lightfoot [4] suggested hollow fibers as possible chromatographic stationary phases, although they considered that problems of fabrication and flow distribution still remained. In 1989, Ding *et al.* [5] verified Gibbs and Lightfoot's suggestion by using a bundle of hollow fibers. They coated the fibers with dodecanol and trioctylphosphate–dodecane and used these systems to separate protein mixtures. Eluent pH values as high as 10 to 11 were used in order to accelerate elution; separation times of about 30 to 80 min were obtained. Ding and Cussler [6] also used such hollow-fiber systems for overloaded chromatography.

The desired characteristics of a stationary phase for liquid chromatography of proteins are well established. The sorbent should have high capacity and a well defined chemistry, and be regenerable and non-denaturing. The stationary phase structure should be rigid, and physically stable at high flow-rates. The material must also be easy to pack and scale up, with defined and reproducible characteristic dimensions. Such properties are usually associated with chromatography columns packed with particulate sorbents. We report another type of material where the stationary phase consists of phenylene phthalamide fibers which have the necessary physical characteristics, as well as separation capabilities. The fibers are assembled into yarns, which in turn are interlaced into a continuous matrix (or fabric). We refer to this as a continuous stationary phase, which when rolled into a cylindrical configuration is readily packed into standard liquid chromatography (LC) columns.

This paper reports packing properties, flow and pressure drop characteristics, protein and activity recovery, loadings for bovine serum albumin (BSA) and β-galactosidase (β-Gal), and the separation of a mixture of immunoglobulin G (IgG), BSA, β-Gal and insulin for an aramid material packed in a rolled, cylindrical configuration.

MATERIALS AND METHODS

Stationary phases

The stationary phase is an aramid fabric obtained from DuPont (Wilmington, DE, USA). It is made from a 95:5 blend of producer-colored olive green T-457 Nomex and producer-colored green Kevlar staple fiber and is finished with an antistatic resin (a mixture of polyglycol alkylamine and epoxy resin), which can be washed off under ordinary laundry conditions [7]. The structures of Nomex, poly(*m*-phenylene isophthalamide), and Kevlar, poly(*p*-phenylene terephthalamide), are shown in Fig. 1 with properties given in Table I. The average fiber length is 45 mm and the fiber width is 10–20 μm. The yarn is a ply of two single yarns with a total width of 200–400 μm.

Aramid is defined by the USA Federal Trade Commission as "a manufactured fiber in which the fiber-forming substance is a long-chain synthetic polyamide in which at least 85% of the amide (CO–NH–) linkages are attached directly to two aromatic rings" [8]. Nomex and Kevlar are DuPont trademarks of fibers that belong to the aramid classification [9,10].

Aramid fibers are highly crystalline, do not melt, and have extremely low combustibility. Their molecular weights are equal to or greater than 60 000, *i.e.*, the degree of polymerization, DP $\geqslant$ 250 [10]. Nomex is noted for its resistance to temperature and flame. The fiber retains useful properties at temperatures up to 370°C [8]. The chemical resistance of aramid fibers is also very good. Nomex is resistant to most alkalis except NaOH at elevated temperatures (60°C) and at concentrations above 50%. It is unaffected by most organic compounds, but is degraded by hot, concentrated acids. Typical uses for Nomex include protective suits for fire fighters and race car drivers, industrial work uniforms,

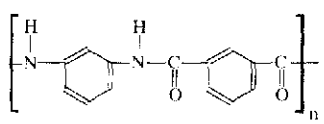

Nomex

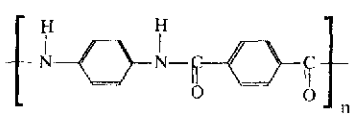

Kevlar

Fig. 1. Chemical structures of Nomex and Kevlar.

TABLE I

CHARACTERISTICS OF ARAMID FIBERS

	Nomex	Kevlar
Specific gravity	1.38	1.44
Tenacity (g/denier) dry	4.8–5.8	21.5
Moisture regain (%)	5.0	3.5–4.5
Burning characteristics	Low flammability	Low flammability
Melting point	Decomposes above 370°C	Decomposes above 260°C
Resistance to:		
Reagents	Degraded by hot, concentrated acid and alkali	Degraded by hot, concentrated acid and alkali
UV light	Degraded after prolonged exposure	Degraded after prolonged exposure

aircraft furnishings, hot gas filtration fabrics and selected components of space vehicles and apparel.

Kevlar aramid fiber has similar resistance to heat (260°C) and chemicals as Nomex. Kevlar has an extremely high tenacity, approximately 22 g/denier, which is more than five times the strength of a steel wire of the same weight and more than twice the strength of industrial nylon, polyester or fiberglass [9]. Kevlar is also flame resistant. End uses for the fiber include tire cord, bulletproof vests, conveyor belts, ropes and cable, fiber reinforcement for aircraft, space vehicles, boats, sports car bodies, and golf clubs. Selected characteristics of aramid fibers are summarized in Table I [8,11].

Packing technique

The fabric is first washed at 70°C in deionized (DI) water, and then air dried. A very small amount of starch is powdered onto the fabric to give it sufficient frictional resistance so that the layers of the fabric will "grab", thus facilitating the rolling of the fabric into a tight cylinder (Fig. 2). Once rolled, plastic ties are placed at 2- to 3-cm intervals to hold the roll in its compact cylindrical form. A hole is punched or drilled through one end of the rolled fabric, and a 10-gauge steel wire is placed through the hole, and bent into place. The wire is then threaded through the chromatography column, and the rolled fabric cylinder is gradually pulled through the column, with the plastic ties being clipped off, one at a time. The fabric is 2 to 5 cm longer than the column, so that when it is pulled through, the end can be cut flush with the column, and the section removed through which the wire was threaded.

The starch is washed out of the column during normal column operation, although some granules were evident in scanning electron micrographs taken after the column had been used.

Liquid chromatography system

To obtain high flow-rates, two pumps (Mini-Pump; Milton Roy, Riviera Beach, FL, USA) are used together in parallel to pump the solvent through an injection valve (Model 7125; Rheodyne,

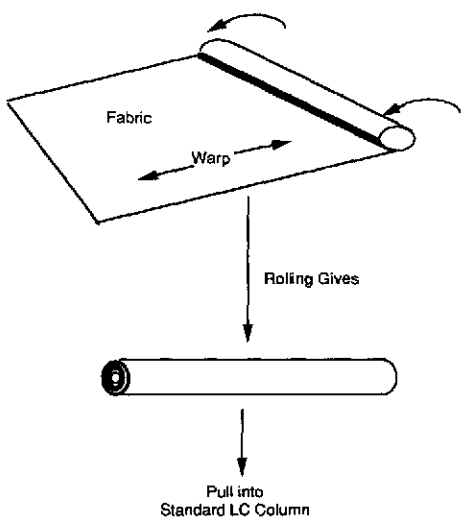

Fig. 2. Schematic representation of rolling and packing procedures.

Berkeley, CA, USA) into the column. The eluent passes into a UV–VIS detector (VARI-CHROM, Sunnyvale, CA, USA) or a refractive index detector (Refracto Monitor Model 1107, Milton Roy) and the signal is recorded on a Linear (Irvine, CA, USA) 1200 chart recorder. The flow-rate used is up to 17.5 ml/min, which is the maximum flow-rate of the combined pumps.

Operational conditions

The columns were run at ambient temperature. Column void volumes were measured with dextran (molecular weight, MW = $2 \cdot 10^6$), polyethylene glycol (PEG 20 000) (both from Sigma, St. Louis, MO, USA) and sodium chloride (from Fisher Scientific, Fair Lawn, NJ, USA). The void fraction based on PEG 20 000 (MW 20 000) was 0.22 and that based on NaCl was 0.37. These values are significantly lower than those obtained for columns packed with spherical particles, where the extra-particle void fraction ranges from 0.35 to 0.40 and the overall void fraction from 0.50 to 0.80.

In order to limit protein consumption, a small column (5 ml in volume) was used for obtaining isotherm, activity, recovery, four-protein separation, and protein loading data. A 46-ml column was also used for some separations to demonstrate the feasibility of packing and using larger columns. The characteristics of both columns are summarized in Table II. This fabric has about 90 000 fibers/g, which corresponds to an external surface area of 0.2 m^2/g.

The pressure drop as a function of flow-rate was measured using the 50-cm column. Stable operation was achieved up to the pumping limit (17.5 ml/min), where the pressure drop was 2000 p.s.i.g. A typical pressure drop curve is shown in Fig. 3.

TABLE II

COLUMN PARAMETERS

	Small	Large
Length (cm)	10	50
Diameter		
O.D. (in.)	3/8	1/2
I.D. (mm)	8.0	10.9
Volume (ml)	5.05	46.3
Stationary phase		
Dry weight (g)	2.68	21.04
Packing density $\left(\frac{\text{g dry stationary phase}}{\text{ml column volume}}\right)$	0.53	0.45

Proteins and eluents

BSA, fraction V powder, anti-human IgG (whole molecule, developed in rabbit), insulin (from bovine pancreas) and β-Gal (grade VIII, from *E. coli*) are all from Sigma. Sodium acetate (80 m*M*, analytical-reagent grade; Mallinckrodt, Paris, KY, USA) and 80 m*M* acetic acid (reagent grade, Fisher) are mixed to give a buffer with pH of 4.7. A concentration of 5 m*M* Na_2HPO_4 (reagent grade; J. T. Baker, Phillipsburg, NJ, USA) is used with 5 m*M* KH_2PO_4 (reagent grade; Matheson, Coleman & Bell, Norwood, OH, USA) to give pH 7.0 buffer, and 10 m*M* $Na_2B_4O_7 \cdot 10H_2O$ (Matheson, Coleman & Bell) is used to adjust pH to 9.2. Ammonium sulfate (purified) is from Baker.

The porosity characteristics were determined using the following molecular probes: ^2H_2O (MW 20); NaCl (58.5); glucose (180); dextran ($2 \cdot 10^6$); and PEGs of molecular weights 200, 300, 400, 600, 1000, 1450, 3350, 8000, 10 000 and 20 000.

β-Gal activity assay

The activity of β-Gal is determined by using *o*-nitrophenyl-β-D-galactopyranoside (ONPG) as substrate. The procedure is as given by Sigma. The absorbance measurement is made 20 min after adding all the reagents.

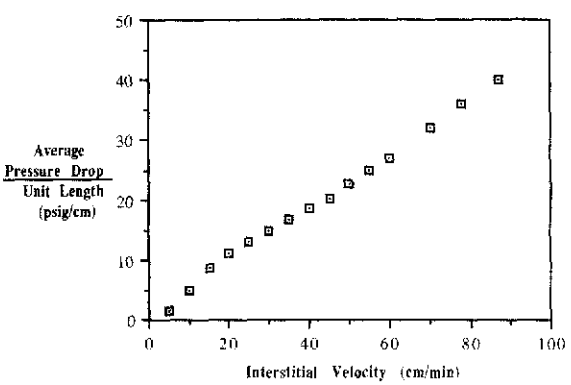

Fig. 3. Characteristic pressure drop of the rolled stationary phase in 50 cm column with aqueous mobile phase at ambient temperature. Column: 50 cm × 10.9 mm I.D., eluent: DI water.

Adsorption isotherm of BSA

The adsorption isotherm of BSA is obtained by frontal analysis [12]. The protein concentration is determined on the LC system with a zero-volume fitting substituted for the column. The concentration is calculated from the peak height using a BSA standard curve. At a concentration of above 2 mg/ml, the relation between peak height and protein concentration is no longer linear. Consequently, breakthrough curves drawn by the chart recorder cannot be used directly for the frontal analysis. In this case, samples are collected, appropriately diluted, and then measured. The adsorption isotherm for BSA in 5 m*M* phosphate buffer (pH 7.0) is monotone and concave-down, with a loading of 4 mg/g at a mobile phase concentration of 5 mg/ml (Fig. 4).

Recovery determination

A stepwise breakthrough–washing–desorption method is used to determine the recovery of protein. If the volume of the breakthrough is V_1 with initial protein concentration of C_0 and emerging concentration of C_1, and if the volume and concentration of protein in the wash step are V_2 and C_2 and in the desorption step are V_3 and C_3, the recovery (R) expressed as a percentage is

$$R(\%) = \frac{C_3 V_3}{C_0 V_1 - (C_1 V_1 + C_2 V_2)} \cdot 100 \qquad (1)$$

Protein recovery was tested with respect to BSA by loading the stationary phase to 4 mg protein/g in 5 m*M* bisodium potassium phosphate buffer at pH 7.0. Elution was achieved by 100 m*M* NaCl (pH 7.0), and the total eluent was collected and analyzed. Protein recovery was 99%.

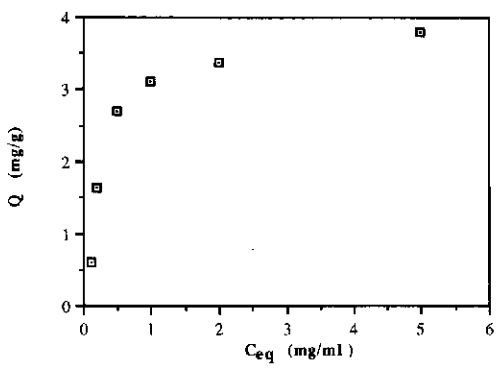

Fig. 4. Adsorption isotherm for BSA. Temperature: 25°C; column size: 10 cm × 8 mm I.D.; flow-rate: 1 ml/min; eluent: DI water.

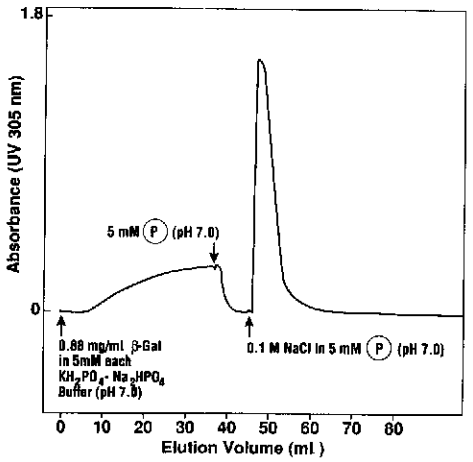

Fig. 5. Adsorption and elution profiles for β-Gal. Temperature: 25°C; column size: 10 cm × 8 mm I.D.; flow-rate: 1.1 ml/min; other conditions indicated in figure. 5 m*M* Ⓟ denotes 5 m*M* Na_2HPO_4–5 m*M* KH_2PO_4.

Retention of enzyme activity was checked by adsorbing β-Gal in 5 m*M* buffer (pH 7.0), and desorbing it at 0.1 *M* NaCl in 5 m*M* phosphate buffer (see Fig. 5). The activity was checked using an ONPG assay before adsorption and after desorption. The β-Gal was from *E. coli* and is a large multimeric protein at pH 7.0 with a molecular weight of 520 000. The adsorption of the β-Gal was much higher than that of BSA, with 0.88 mg/ml of β-Gal giving a loading of 6.1 mg/g stationary phase. The β-Gal capacity at higher concentrations was not determined because of the expense involved. Desorption of the β-Gal gave complete recovery of specific activity based on the ONPG assay.

Plate height determination

Plate heights were determined using the 50-cm column. Samples of PEG 20 000, PEG 200, or ^2H_2O (volume 100 μl) were injected and eluted from the column. Plate height was calculated directly from the chromatogram, with peak width measured at half-height.

RESULTS

Separations

This stationary phase is capable of separating both small and large proteins as indicated by the fractionation of IgG (MW 146 000–165 000), BSA (MW 60 000), insulin (MW 6100 for monomer, 12 200 for dimer), and β-Gal (MW 520 000), shown in Fig. 6. The multimodel nature of this stationary phase is related to its structure (Fig. 1) and possibly to the dye in the fiber. The polymers in the aramid fabrics have amino and/or carboxyl end groups, depending on how the polymerization was quenched, and thus exhibit ionic character. The aromatic polyamides also have many benzene rings. Hydroxylated adsorbates may therefore form π bonds with the benzene rings and adsorb.

The effect of both ionic and hydrophobic interactions between aramid fibers and proteins can be explained through Table III which summarizes retention characteristics for the four proteins in five different eluents. All four proteins studied in this paper are strongly retained in the column using DI water as eluent but unretained in 0.1 *M* NaCl. When 1 *M* $(NH_4)_2SO_4$ is the eluent, two of the proteins, insulin and β-Gal, are still strongly retained. This indicates that, in addition to ionic interactions, insulin and β-Gal exhibit hydrophobic interactions [13].

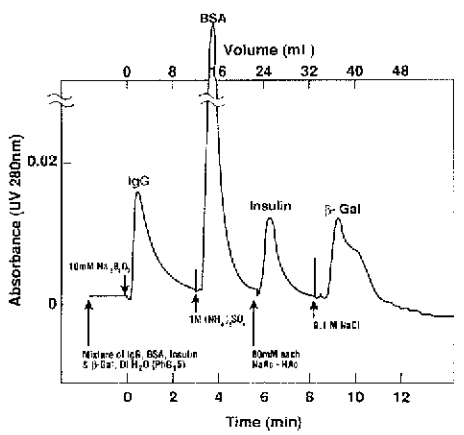

Fig. 6. Separation of four-protein mixture at flow-rate of 4 ml/min and ambient temperature (small column). Injection volume of 200 μl with the proteins at concentrations of 10 mg/ml (IgG), 10 mg/ml (BSA), saturated (insulin), and 4 mg/ml (β-Gal) (pH 7.0). Ac = Acetyl.

TABLE III

STEPWISE DESORPTION PROTOCOL

+ = Retained; − = unretained.

Eluent	Protein			
	IgG	BSA	Insulin	β-Gal
DI Water (pH 5.5)	−	+	+	+
10 m*M* $Na_2B_4O_7$ (pH 9.2)	−	+	+	+
1 *M* $(NH_4)_2SO_4$ (pH 4.5)	−	−	+	+
80 m*M* NaAc–80 m*M* HAc (pH 4.7)	−	−	−	+
0.1 *M* NaCl (pH 5.5)	−	−	−	−

Porosity

Scanning electron microscopy (SEM) compares the structures of the flat and rolled materials (Fig. 7a and b). SEM of the flat material (Fig. 7a and c) shows yarns having a diameter of 200–400 μm, with each yarn consisting of many fibers having a diameter of 10–20 μm. When rolled (Fig. 7b) a tightly packed three-dimensional matrix results. Void volumes which are accessible to eluent flow are shown in the schematic diagram of Fig. 8 and include the space between fibers, yarns and intermatrix voids.

The SEM and fiber characteristics lead to the definition of three porosities: (1) between the yarns, or the interyarn porosity with a void fraction ε_b; (2) between the fibers within a yarn or the interfiber porosity (ε_p); and (3) intrafiber void fraction (ε_i) from pores and cracks within each fiber, enclosed areas that arise when the fibers are twisted around each other to form a yarn, and from the crossing of yarns. This description is analogous to a column packed with particles possessing a macro- as well as a microporosity; ε_b, ε_p, and ε_i then correspond, respectively, to the interstitial, macroporous and microporous void fractions.

The flow porosity is about 0.22 based on the elution volume of PEG 20 000. This is low compared even to the external porosity generated by the dense packing of non-porous spherical particles, which is theoretically 0.26 [14,15], although in practice values around 0.40 are obtained. Since the

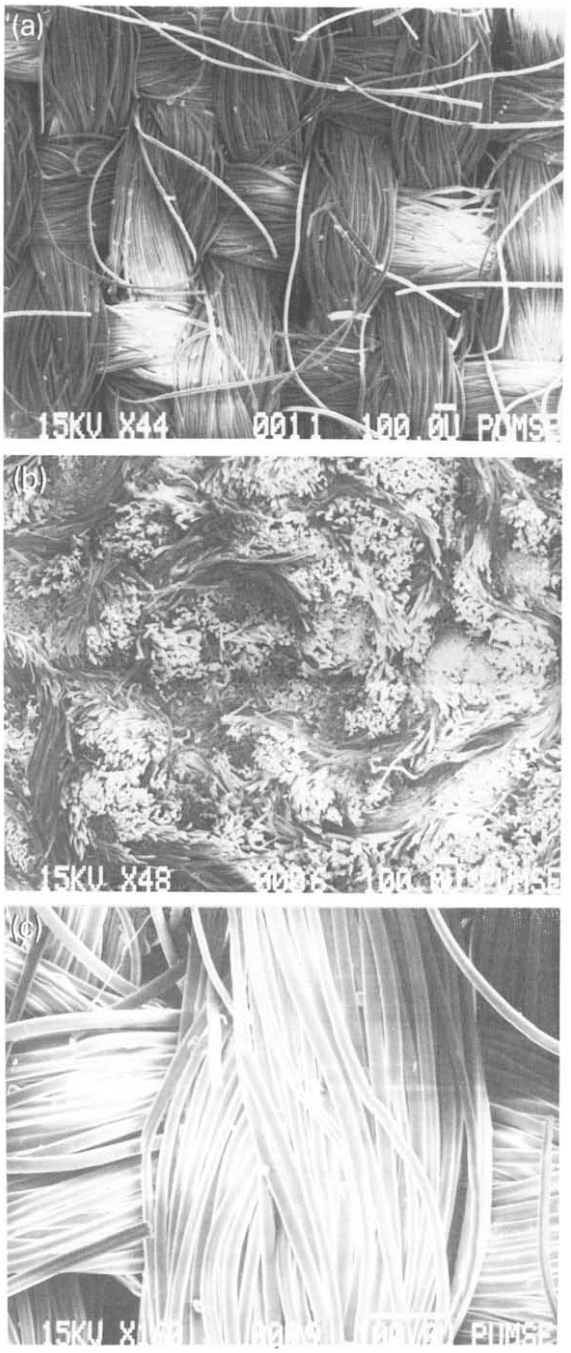

Fig. 7. Scanning electron micrographs of (a) flat fabric, (b) cross-section of rolled fabric, (c) yarn, showing individual fibers. Scale indicated at bottom of picture, bar = 100 μm.

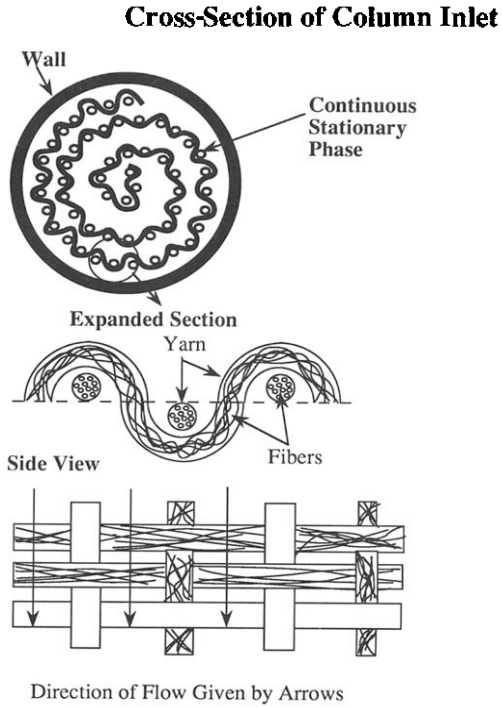

Fig. 8. Schematic of the rolled stationary phase within the column.

fabric is compressed during column packing, the measured void fraction will be lower than the overall permeabilities reported in the textile literature, which were obtained by batch measurements [16–19].

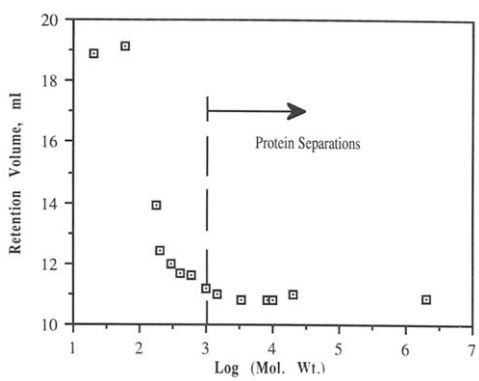

Fig. 9. Elution volume as a function of probe molecular weight. Temperature: 25°C; column size: 50 cm × 10.9 mm I.D.; flow-rate: 1.0 ml/min; eluent: DI water. The probes used were NaCl (MW 58.5); ^2H_2O (MW 20); glucose (MW 180); PEGs of molecular weight 200, 300, 400, 600, 1000, 1450, 3350, 8000, 10 000 and 20 000; and dextran (MW $2 \cdot 10^6$).

A series of molecular weight probes gave the retention behavior of Fig. 9. At molecular weights greater than 1000, the retention volume is essentially independent of molecular weight. These probes see all of the interyarn and interfiber spaces. The smaller probes (MW < 1000) also see some part of the intrafiber pore space. Because of the relatively large interfiber diameters (Fig. 7b and c), even the largest probes see all of the interfiber space, unlike in conventional chromatography with packed particles, where the macroporous space need not be completely accessible to the largest probes.

Pressure drop

Applied pressure drop is a linear function of velocity over the entire experimental range of flow-rates (Fig. 3), and follows Darcy's law (see refs. 20 and 21).

Modified Van Deemter equation

The scanning electron micrographs of Fig. 7 show relatively large interfiber spaces (on the order of micrometers). Thus convection is likely to occur through both interyarn and interfiber channels, as illustrated schematically in Fig. 10. The interfiber channels have a small cross-sectional area while the interyarn channels are large. Just as flows in parallel pipes of equal lengths distribute according to cross-sectional areas, flow through these channels are envisioned to distribute in proportion to their cross-sectional areas. Consequently, pore (*i.e.*, interfiber) velocity, v_{pore}, is a small fraction of the interyarn velocity, and therefore of the chromatographic velocity, v_{chrom}. As the eluent flow-rate increases, both the pore and the chromatographic velocity will increase proportionately (their ratio will remain constant, independent of flow-rate). At higher flow-rates, the pore velocity could become high enough to make convective transport through the interfiber space appreciable relative to diffusive transport. This would in turn affect the overall plate height expression. In order to estimate the contribution of convective intrafiber transport to band-spreading, we make the simplifying assumption of plug flow. Then the effects of convection and diffusion can be added in parallel after Guttman and DiMarzio [22]. The convective contribution to plate height for piston flow is independent of velocity; thus, the total plate height due to the "intraparticulate" pore space is given by:

$$\frac{1}{H_{pore,\,total}} = \frac{1}{H_{conv}} + \frac{1}{H_{diff}} = \frac{1}{D} + \frac{1}{C' v_{pore}} \qquad (2)$$

where C' and D are empirical parameters. Eqn. 2 can be rewritten as

$$H_{pore,\,total} = \frac{DC' v_{pore}}{D + C' v_{pore}} \qquad (3)$$

At high velocities, the convective term dominates the expression, while the opposite is true at low flows. The total plate count is then given by

$$H_{total} = A + \frac{B}{v_{chrom}} + \frac{DC v_{chrom}}{D + C v_{chrom}} \qquad (4)$$

which is the modified Van Deemter equation applicable to systems involving flow through the particles. Here, the pore velocity is replaced by the chromatographic velocity ($v_{pore} = f v_{chrom}$ where $0 < f < 1$). The additional constant, f, has been absorbed into C' to give C. Note that the chromatographic velocity [23] will be different for probes that see different fractions of the total mobile phase space.

Eqn. 4 gives the solid line fit to the data using non-linear regression in Figs. 11 and 12, where the reduced plate height h, given by H_{total}/d_W, is used. An average value of 300 μm was used for the characteristic particle size (yarn width) d_W. Table IV compares values of A, B, C and D for the classical and modified Van Deemter equations. The modified

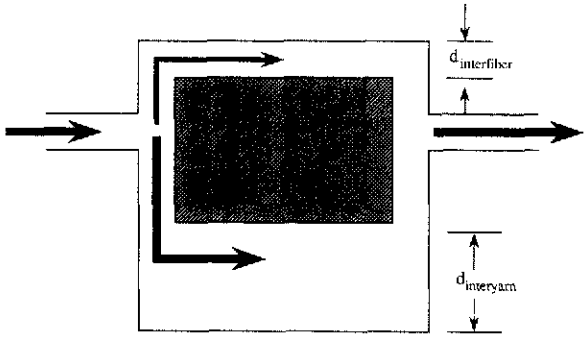

Fig. 10. Schematic of the parallel flow patterns available, representing flow through the interyarn and interfiber channels. There are numerous interfiber channels for every interyarn channel but the diagram only shows one channel of each kind, for simplicity.

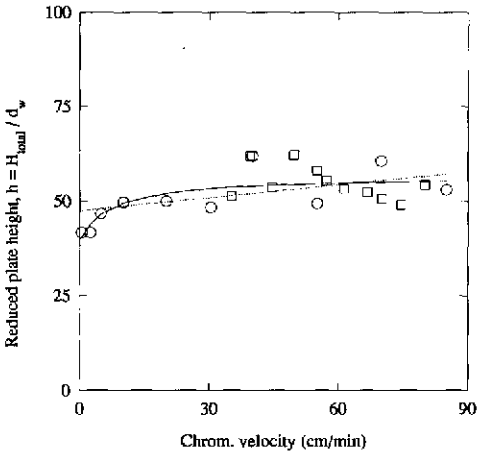

Fig. 11. Plate height as a function of chromatographic (Chrom.) velocity for PEG 20 000. The symbols ○, □ represent two different experimental runs; the dotted line represents the best-fit Van Deemter expression, and the continuous line the best-fit modified Van Deemter expression.

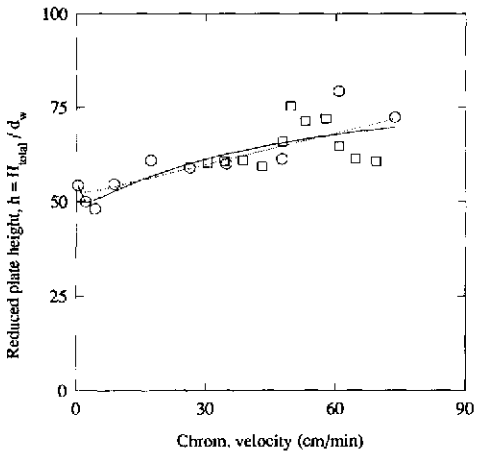

Fig. 12. Plate height as a function of chromatographic velocity for PEG 200. Symbols as in Fig. 11.

Van Deemter equation follows the trend of the data over the entire range of chromatographic velocities [$= Q/(A_x\varepsilon_i')$].

For PEG 20 000, the contribution due to convection within the interfiber pores dominates the contribution of diffusion at high velocities, giving the flat plate height line in Fig. 11. The velocity range in which axial dispersion dominates bandspreading is lower than that used in the present experiments, and consequently the plate height data do not show a minimum. The modified Van Deemter equation fits the data well over the entire velocity range. At high enough velocities, eqn. 4 reduces to

$$H_{\text{total}} \approx A + D \tag{5}$$

which corresponds to the flat region for velocities above 30 cm/min in Fig. 11.

TABLE IV

COMPARISON OF FITTED CONSTANTS FOR CONVENTIONAL AND MODIFIED VAN DEEMTER EQUATIONS

Data in Figs. 11 and 12 fitted by non-linear regression using the Marquardt method (the NONLIN procedure in the statistical package SAS). Parentheses contain values of asymptotic standard error.

	PEG 200		PEG 20 000	
Average molecular weight	200		20 000	
Estimated D (cm^2/s)[a]	$6.3 \cdot 10^{-6}$		$8.5 \cdot 10^{-7}$	
Conventional Van Deemter ($h = A + B/v_{\text{chrom}} + Cv_{\text{chrom}}$)				
A	51.5	(2.98)	47.4	(2.36)
B	0.81	(2.69)	0.0	–
C	0.28	(0.063)	0.11	(0.045)
Modified Van Deemter (eqn. 4)				
A	46.7	(6.02)	39.3	(5.29)
B	3.0	(3.54)	0.0	–
C	0.77	(0.75)	2.5	(3.28)
D	38.5	(18.8)	17.3	(4.68)

[a] Estimated using the Wilke–Chang equation (see ref. 24).

Unlike PEG 20 000, which is too large to penetrate pores inside the fibers, PEG 200 is small enough to explore some of the intrafiber, as well as all of the interfiber and interyarn spaces. Thus, for PEG 200 the plate height increases slightly even at the highest velocities (Fig. 12). There is a plate height contribution due to microporous diffusion which, in contrast to diffusion in the interfiber space, does not act in parallel with any convective term. (There is no flow through the micropores, which are taken to be closed.) Thus the microporous diffusion contribution is linearly proportional to the velocity [25]. In addition, the smaller size of PEG 200 (and consequently its higher diffusivity) implies that the velocity range over which axial dispersion is dominant would be higher than that for PEG 20 000. In fact, this region is accessed over the experimental velocity range, and a minimum is seen in the data.

A result which did not fit either the modified Van Deemter (eqn. 4) or the classical equation was obtained for deuterated water. The ^2H_2O was found to give a decreasing plate height with increasing velocity (Fig. 13). It was expected that ^2H_2O would give a greater increase in plate height than PEG 200, since ^2H_2O is capable of exploring a bigger fraction of the microporous space.

It is not clear what causes the decreasing plate height. We hypothesize that at low flow-rates mass transfer contributes to the overall plate height due to an external boundary layer between interstitial and interfiber pores. However, at higher flow-rates, where convection becomes the dominant interfiber transport mechanism, contributions due to mass transfer across a boundary layer could be decreased, thus decreasing the overall plate height as described by Van Kreveld and Van den Hoed [25]. This would be particularly noticeable for ^2H_2O, which as a small molecule has a diffusivity on the order of $33 \cdot 10^{-6}$ cm^2/s compared to $6.3 \cdot 10^{-6}$ for PEG 200 and $8.5 \cdot 10^{-7}$ for PEG 20 000 [24].

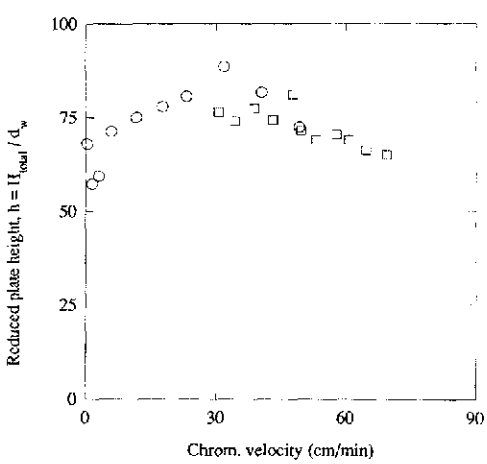

Fig. 13. Plate height as a function of chromatographic velocity for ^2H_2O. Symbols as in Fig. 11. Neither the Van Deemter nor the modified Van Deemter curves are shown because they fit the data poorly, for reasons explained in the text.

DISCUSSION

Other workers have considered analogues to the "coupling" between flow and diffusion described above. For size-exclusion chromatography, Van Kreveld and Van den Hoed [25], considered that eddy diffusion would extend from the interstitial space into the intraparticulate pores, although not necessarily fully penetrating the pore. Here the pores are not assumed to traverse the entire particle. They therefore added a velocity-dependent correction, D^*v to the pore diffusivity, D_p, to obtain an effective diffusivity:

$$D_{p,eff} = D_p + D^*v \tag{6}$$

where D^* is due to eddies. They reported a plate height expression having axial dispersion, eddy diffusion, and convective terms:

$$H_{total} = \frac{2D_m}{v} + 2A + \frac{k'}{30(1+k')^2}\left\{\frac{vd^2_{particle}}{D_p + D^*v}\right\} \tag{7}$$

This is similar in form to eqn. 4. The second term, $2A$, in eqn. 7 is due to eddy diffusion and the last term is the combined effect of flow and diffusion within the particle where the external mass-transfer contribution is neglected. At low velocities, the diffusive contribution ($2D_m/v$) predominates, and plate height is inversely proportional to the linear velocity. At high velocities, the convective term dominates, resulting in a velocity-independent plate height contribution $\{(k'/[30(1+k')^2]\}(d^2_{particle}/D^*)$.

A similar approach is described by Afeyan *et al.* [26] who report a form of chromatography where flow occurs through the particle (which they term

"perfusion chromatography"). They use a correction to the intraparticulate diffusivity analogous to eqn. 6:

$$D_{p,eff} = D_p + \frac{d_{particle}\, v_{pore}}{2} \quad (8)$$

This again results in a velocity-independent plate height contribution at high flow-rates, as in eqn. 7.

These approaches, in which two mechanisms act "in parallel," are similar to the coupling theory of Giddings [27] in which contributions from flow and diffusion act simultaneously. However, as has been pointed out by Van Kreveld and Van den Hoed [25], when flow occurs across a particle, the coupling between diffusive and convective transport across the particle becomes significant over a much higher range of flow-rates than the coupling described by Giddings.

CONCLUSIONS

The concept of LC using a continuous stationary phase, rolled and inserted into a standard LC column, is demonstrated. This stationary phase has the desirable attributes of mechanical stability and high selectivity and recovery; it is non-denaturing, and has potential for preparative protein separations if higher capacities are attained. The plate height is nearly constant at high chromatographic velocities for a solute which is small enough to pass through pore spaces which transverse the stationary phase matrix, but large enough to be excluded from the smaller dead-end pores. A coupling argument based on simultaneous flow and diffusion is used to explain this effect, and a modified Van Deemter expression is proposed which may be useful in describing other types of stationary phases with transecting pores.

ACKNOWLEDGEMENTS

The material in this work was supported by NSF Grants 8907304 and BCS 8912150. We thank R. Hendrickson, K. Kohlmann, and D. McCabe for experimental assistance. We also express our appreciation to G.-J. Tsai and A. Sarikaya and Dr. R. Dean for their helpful comments during preparation of this manuscript.

SYMBOLS

A	Eddy diffusion contribution to plate height, cm
A_x	Empty column cross-sectional area, cm^2
B	Coefficient of axial dispersion term in Van Deemter expressions (eqn. 4), cm^2/s
C	Coefficient of linear velocity term in the modified Van Deemter expression (eqn. 4), s
C'	Empirical parameter representing constant for convection through pores, s
C_1	Effluent protein concentration during breakthrough, mg/ml
C_2	Concentration of protein during wash step, mg/ml
C_3	Concentration of protein during desorption step, mg/ml
C_0	Initial protein concentration
C_{eq}	Equilibrium concentration of protein, mg/ml
D	Additional term in modified Van Deemter expression (eqn. 4), representing H_{conv}, cm
D^*	"Eddy diffusivity" corresponding to flow within particles (eqn. 6), cm
D_m	Molecular diffusivity, cm^2/s
D_p	Pore diffusivity, cm^2/s
$D_{p,eff}$	Effective pore diffusivity incorporating convective effects (eqn. 6), cm^2/s
$d_{interfiber}$	Characteristic diameter of interfiber space, cm
$d_{interyarn}$	Characteristic diameter of interyarn space, cm
$d_{particle}$	Particle diameter, cm
d_w	Characteristic distance (yarn width) for convection and diffusion in the interfiber channels, cm
f	fraction of interstitial flow-rate which passes through the pores, dimensionless
h	Reduced total plate height, H_{total}/d_w, dimensionless
H_{conv}	Contribution to plate height from convection through the interfiber channels, cm
H_{diff}	Contribution to plate height from diffusion through the interfiber channels, cm

$H_{pore,\ total}$	Net contribution from within the interfiber channels to the overall plate height, cm
H_{total}	Total plate height, cm
k'	Capacity factor (dimensionless)
Q	Volumetric flow-rate, ml/min
R	Recovery of protein
V_1	Volume of the breakthrough, ml
V_2	Volume of effluent during wash step, ml
V_3	Volume of effluent during desorption step, ml
v	Linear velocity, cm/s
v_{chrom}	Chromatographic velocity, cm/s
v_{pore}	Interfiber velocity, cm/s
V_R	Retention volume, ml

Greek symbols

ε_b	Interyarn void fraction, dimensionless
ε_i	Intrafiber void fraction, dimensionless
ε_i'	Void fraction seen by non-interacting component i, dimensionless
ε_p	Interfiber void fraction, dimensionless

REFERENCES

1 H. B. Reisman, *Economic Analysis of Fermentation Processes*, CRC Press, Cleveland, OH, 1988, p. 75.
2 G. K. Sofer and L.-E. Nystrom, *Process Chromatography*, Academic Press, San Diego, CA, 1989, p. 107.
3 P. Knight, *Bio/Technology*, 7 (1989) 777.
4 S. J. Gibbs and E. N. Lightfoot, *Ind. Eng. Chem. Fundam.*, 25 (1986) 490.
5 H. Ding, M-C. Yang, D. Schisla and E. L. Cussler, *AIChE J.*, 35 (1989) 814.
6 H. Ding and E. Cussler, *Biotech. Prog.*, 6 (1990) 472.
7 D. E. Hoffman, Industrial Products Division, Fibers and Composites Development Centers, E. I. DuPont de Nemours and Company, Wilmington, DE, personal communication, September (1989).
8 Federal Trade Commission, *Rules and Regulations Under the Textile Fiber Products Identification Act*, Washington, DC, July 9, 1986.
9 M. L. Joseph, *Introductory Textile Science*, Holt, Rinehart & Winston, New York, 5th ed., 1986, p. 110.
10 J. Preston, in M. Grayson (Editor), *Kirk-Othmer Encyclopedia of Chemical Technology*, Vol. 3, Wiley, New York, 3rd ed., 1978, p. 213.
11 P. G. Tortora, *Understanding Textiles*, Macmillan, New York, 5th ed., 1992, p. 188.
12 J. R. Conder and C. L. Young, *Physico-Chemical Measurements by Gas Chromatography*, Wiley, Chichester, 1979, Ch. 9.
13 B. F. Roettger and M. R. Ladisch, *Biotech. Adv.*, 7 (1989) 15.
14 R. M. German, *Particle Packing Characteristics*, Metal Powder Industries Federation, Princeton, NJ, 1989, pp. 32–34, 89–97.
15 D. J. Cumberland and R. J. Crawford, *The Packing of Particles*, Elsevier, Amsterdam, 1987, pp. 14–18.
16 R. McGregor, *J. Soc. Dyers Colour.*, 81 (1965) 429.
17 L. D. M. van den Brekel and E. J. de Jong, *Textile Res. J.*, 59 (1989) 433.
18 L. D. M. van den Brekel and E. J. de Jong, *Textile Res. J.*, 60 (1990) 429.
19 P. Banks-Lee, H. Peng and M. Mohammadi, *Textile Res. J.*, 60 (1990) 427.
20 A. E. Scheidegger, *The Physics of Flow Through Porous Media*, University of Toronto Press, Toronto, 3rd ed., 1974, pp. 73–79.
21 G. I. Barenblatt, V. Entov and V. M. Ryzhik, *Theory of Fluid Flows Through Natural Rocks*, Kluwer, Dordrecht, 1990, pp. 9–12.
22 C. M. Guttman and E. A. DiMarzio, *Macromolecules*, 3 (1970) 681.
23 Cs. Horváth and H.-J. Lin, *J. Chromatogr.*, 126 (1976) 401.
24 R. C. Reid, J. M. Prausnitz and T. K. Sherwood, *The Properties of Liquids and Gases*, McGraw-Hill, 3rd ed., 1977, pp. 567–590.
25 M. E. van Kreveld and N. van den Hoed, *J. Chromatogr.*, 149 (1978) 71.
26 N. B. Afeyan, N. F. Gordon, I. Maszaroff, L. Varady, S. P. Fulton, Y. B. Yang and F. E. Regnier, *J. Chromatogr.*, 519 (1990) 1.
27 J. C. Giddings, *Dynamics of Chromatography*, Part I, Marcel Dekker, New York, 1965, pp. 47–61.